19 June 1970, Volume 168, Number 3938 SCIENCE

Nuclear Fission Revisited

Nuclear shells introduce structure into the fission barrier and lead to a number of interesting phenomena.

John R. Huizenga

Immediately after the discovery of nuclear fission by Hahn and Strassmann (*1*), Bohr and Wheeler (*2*) presented an outstanding paper on the theory of fission. In this classic paper the authors treated the nucleus in a fashion analogous to a charged liquid drop with two opposing forces controlling the nuclear stability. Long-range Coulomb forces between the protons act to disrupt the nucleus, whereas short-range nuclear forces, idealized as a surface tension, act to stabilize the nucleus. The degree of stability of a nucleus is the result of a delicate balance between the weak electromagnetic forces and the strong nuclear forces. Although each of these forces is several hundred million electron volts for a heavy nucleus, a typical fission barrier is only 5 million electron volts. Investigators have used this charged liquid-drop model with great success in describing the general features of nuclear fission and also in reproducing the total nuclear binding energies. Extensive studies of the deformation energy of such a charged liquid drop have been made in recent years (see *3*).

It has been known for some time, however, that there are marked deviations from the predictions of the liquid-drop model in the total nuclear binding energies in the vicinity of the well-known neutron and proton shells (*4*). Recently it has been suggested (*5*) that nuclear shells give rise also to structure in the liquid-drop fission barrier of some nuclei. Since the typical fission barrier is only a few million electron volts, the magnitude of the shell corrections needs only to be small in order that irregularities be introduced in the barrier. This structure is illustrated by the solid line in Fig. 1 for ^{240}Pu where the fission barrier has two maxima with a rather deep minimum in between. For comparison, the liquid-drop barrier is schematically illustrated by the dashed line in Fig. 1. The two-humped barrier will be discussed in this article in terms of the inner barrier *A* and the outer barrier *B*.

Although fission is an exothermic process, the lifetime for spontaneous fission decay from the ground state is very long. This is so because of the fission barrier. In the initial stages of deformation the potential energy increases. However, at a particular nuclear shape additional deformation leads to an increase in the surface energy which exactly balances the decrease in the Coulomb energy. This configuration of maximum potential energy is referred to as the "saddle point" or "transition nucleus." The analogous configuration in chemical reactions is referred to as a "transition state" or an "activated complex." The saddle point is a configuration of special importance in fission theory. In a manner analogous to the calculation of chemical reaction rates, Bohr and Wheeler (*2*) first computed fission reaction rates by the transition state method.

In this article I shall discuss the experimental evidence for a double-humped barrier and some of its characteristic consequences, as well as the theoretical basis for this barrier structure as first proposed by Strutinsky (*5*). In addition, some features of the scission and postscission stages of the fission process will be discussed.

Spontaneously Fissionable Isomers

The discovery of spontaneously fissionable isomers (*6*) initiated a new wave of interest in fission. Suitable theoretical explanation for these isomers was lacking until Strutinsky (*5*) suggested the existence of a second minimum in the potential energy surface as illustrated in Fig. 1. In terms of the theoretical explanation for the isomers the problem demands, on the one hand, that one account for the enormous enhancement in the fission decay of the isomers relative to the spontaneous fission decay of the ground state (by a factor of approximately 10^{20}, an indication of an excitation energy of some 2 or 3 million electron volts) and, on the other hand, that one formulate a mechanism that gives sufficient retardation to the gamma-ray decay of the isomer. Explanation of the initially discovered americium (odd proton–odd neutron isotopes) isomers in terms of the coupling of specific Nilsson orbitals with high angular momentum proved to be unacceptable as more information about the yields and energies of the isomers became available. In addition, as more heavy nuclei were investigated, fissionable isomers became the rule rather than the exception for certain values of atomic number *Z* and mass number. A listing of fissionable isomers in the elemental region from uranium to curium is given in Table 1.

The author is professor in the Department of Chemistry and in the Department of Physics and is a member of the staff of the Nuclear Structure Research Laboratory, University of Rochester, Rochester, New York 14627.

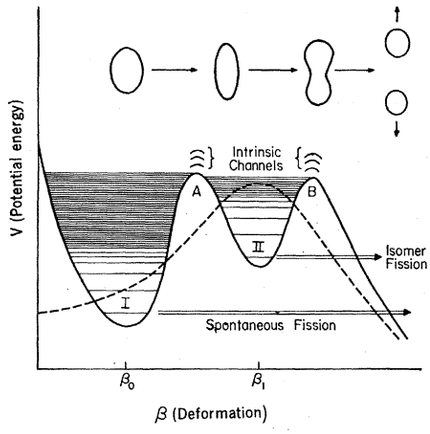

Fig. 1. Schematic illustrations of single-humped (dashed line) and double-humped (heavy solid line) fission barriers. Intrinsic excitations in the first and second wells at deformations β_0 and β_1 are designated as class I and class II states, respectively. Intrinsic channels at the two barriers are also illustrated. The transition in the shape of the nucleus as a function of deformation is schematically represented in the upper part of the figure. Spontaneous fission of the ground state and isomeric state occur from the lowest energy class I and class II states, respectively.

The lifetimes range from nanoseconds to several milliseconds, a time range quite accessible to experiment. The evidence for an isomer (*7*) of ^{241}Pu with a half-life of 0.3 year is tentative. Although isomers decaying by spontaneous fission have been reported also in other parts (*8*) of the periodic table, some uncertainty remains about both their existence and the reason for their existence.

The Franck-Condon principle states that nuclei excited into the minimum between the two barriers are stable toward decay by direct radiative transitions to the ground state. A change in the nuclear shape is required prior to gamma-ray decay and, hence, the hindrance introduced by the penetration through barrier *A* is in accord with the relative stability of the isomers toward decay by radiation. On the other hand, the large enhancement in the decay of the isomer by fission relative to the spontaneous fission decay of the ground state is accounted for by the smaller barrier of the isomer and the extreme sensitivity of the penetrability of the barrier to its magnitude. The spontaneously fissioning isomeric states are the ground states in the second potential well and represent the zero-point vibration coupled to the lowest intrinsic state at the deformation of the second well.

Compound Nucleus Resonance States

Recent measurements of the subthreshold neutron fission cross sections of several nuclei have revealed groups of fissioning resonance states with wide energy intervals between each group where no fission occurs. Such a spectrum is illustrated in Fig. 2 where the subthreshold fission cross section (*9*) of ^{240}Pu is shown for neutron energies between 500 and 3000 electron volts. In between the groups of fissioning resonance states, there are many other resonance states known from data on the total neutron cross sections but these have negligible fission cross sections. These data can be explained in terms of the two-humped fission barrier.

In Fig. 1 the deformation β_0 represents the ground state of a heavy nucleus that is known to be deformed. The deformation β_1 represents the minimum potential energy between barriers *A* and *B*. If the relative potential energy at deformation β_1 is higher than that at β_0, the density of excitation levels at deformation β_0 is larger than that at β_1 for a given excitation energy *E*. The levels in the second well then act as intermediate states as the fissioning nucleus goes from the initial compound nuclear resonance states in the first well to scission. The mechanism for slow neutron subbarrier fission is postulated to proceed in the following way (*10*, *11*). The interaction of a slow neutron with the target nucleus produces a compound nucleus with deformation β_0 in one of the class I levels with a particular excitation energy *E*. This energy is the sum of the neutron binding energy and the neutron kinetic energy. By variation of the neutron kinetic energy, different compound resonance states of deformation β_0 are reached. Each of the compound resonance states decays by one or more of the available exit channels (emission of gamma rays, emission of neutrons, and fission). However, if and only if the energy of the class I state at β_0 accidentally is almost equal to the energy of a class II state at β_1 will the nucleus undergo a transition from the compound nuclear level to the intermediate state, which, in turn, may fission with a high probability. Such a mechanism gives rise to groups of fissioning resonance states, like those shown in Fig. 2, where each group corresponds to one of the intermediate states at β_1 which have been designated as class II states.

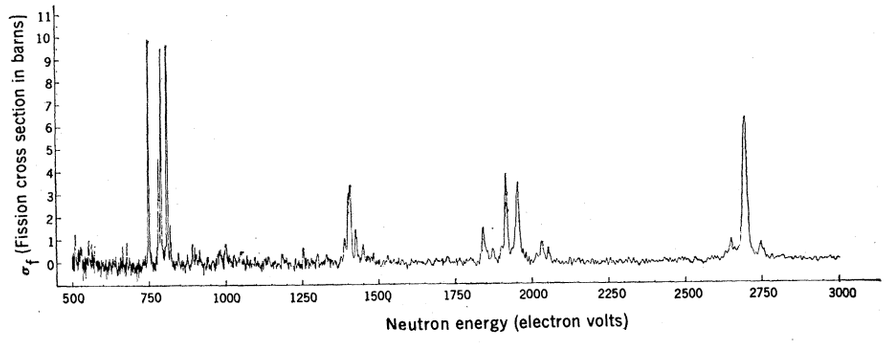

Fig. 2. The subthreshold neutron fission cross section (*9*) of ^{240}Pu between 500 and 3000 electron volts.

Vibrational Resonance States

The excitation function for the fission of ^{230}Th induced by neutrons (*12*, *13*) has an unusual maximum for neutron energies in the vicinity of 700 kiloelectron volts as illustrated in Fig. 3. Detailed calculations (*11*, *12*) have shown that no reasonable assumptions about competing decay modes, such as inelastic neutron scattering, can explain satisfactorily the observed maximum of the fission cross section which is in an energy region where the fission cross section is expected to increase exponentially. Therefore, it has been suggested that the maximum may be associated with a vibrational-mode resonance state. If the second well is shallow, a well-developed vibrational level is expected to exist in this well. Additional evidence for such resonance states has come from neutron fission induced by the deuteron stripping (d,pf) reaction (*14*) at energies below the neutron binding energy where the maxima cannot be associated with neu-

tron evaporation. The fine structure observed in the fission probability at an excitation of 5 million electron volts in the ^{239}Pu(d,pf) reaction (*15*) is especially suggestive of some type of resonance in the second well.

The vibrational states in the first well are expected to be separated from each other by about 1 million electron volts. The strength of such a state in a nucleus excited to some 5 million electron volts (near the top of the fission barrier) will spread over the compound states with a width of the order of 1 million electron volts. Hence, in the model of fission with one potential well, the vibrational-mode resonance states are not expected to occur. If the minimum in the second well has a higher energy than that of the first well, this makes it possible for one to observe vibrational states in fission (*11*, *16*). Now it may happen that a collective vibrational level near the top of the barrier in the first well is the ground state or a low-lying excited state in the second well. The fission cross section will reflect vibrational resonance states whenever there are excitations in the nonfission degrees of freedom with appropriate spin and parity coupled to the vibrational states, the only restriction being that the level width is smaller than the level spacing. The spontaneously fissioning isomers are probably the best examples of vibrational states in the second well that are essentially unmixed with other states in the second well.

Fission Fragment Angular Distributions

Bohr (*17*) suggested that the angular distributions of the fission fragments are explainable in terms of the transition state theory. The theory predicts that the cross section will have a steplike behavior for energies near the fission barrier, and that the angular distribution will be determined by the quantum numbers associated with each of the specific fission channels. The relationship between the quantum numbers J, M, and K is illustrated in Fig. 4. The parity π is conserved throughout the fission process.

The theoretical angular distribution of the fission fragments is based on two assumptions (*17*). First, the two fission fragments are assumed to separate along the direction of the nuclear symmetry axis so that the angle θ represents the angle between the body-fixed axis and the space-fixed axis. Second, it is assumed that the transition from the saddle point to scission is so fast that the Coriolis forces do not change the values of K established at the saddle point. One of the simplest tests of this model has been a study of the photofission (fission induced by gamma rays) of even-even targets. Dipole absorption predominates so that the spin and parity of the compound states are 1−, and with the space-fixed axis along the photon direction, $M = \pm 1$. The theoretical angular distribution for transition states $K = 0$ and $K = 1$ is given by

$$W(\theta) = a + b \sin^2\theta \qquad (1)$$

where the coefficients a and b are related to the relative contributions of $K = 0$ and $K = 1$ states. Experimental results from the photofission of even-even targets near the fission barrier

Table 1. Spontaneously fissionable isomers.

Mass number	Half-life (nanoseconds)	Method of production	Reference	Isomeric energy (Mev)
		Uranium		
234	33 ± 5	(n,γ)	(*44*)	
234	< 4	(d,p)	(*45*)	
234	< 2	(α,2n)	(*46*)	
235	20 ± 5	(n,γ)	(*44*)	2.7 (*11*)
236	110 ± 50	(d,p)	(*47*)	
236	67 ± 9	(n,γ)	(*44*)	
236	105 ± 20	(d,pn)	(*46*)	
236	70 ± 20	(d,p), (d,pn)	(*48*)	
238	300 ± 100	(d,pn)	(*45*)	
238	195 ± 30	(d,pn)	(*46*)	
238	110 ± 30	(d,pn)	(*48*)	
239	< 3	(n,γ)	(*44*)	
		Neptunium		
No isomers observed with half-lives from 1 nanosecond to several hours and formation cross sections greater than 10^{-7} barn in 12-Mev proton and deuteron bombardments of ^{233}U, ^{234}U, ^{235}U, ^{236}U, ^{238}U [(*45*) and other references]				
		Plutonium		
235	20	(α,2n)	(*49*)	
235	30 ± 5	(α,2n)	(*50*)	3.0 ± 0.2 (*50*)
236	34 ± 8	(p,2n)	(*47*)	3.7 (*47*, *51*)
237	120	(α,2n)	(*52*)	
237	100 ± 30	(d,2n)	(*47*)	
237	120 ± 50	(α,2n)	(*50*)	3.4 ± 0.2 (*50*)
237	900	(d,2n)	(*45*)	
238	< 2	(α,4n)	(*52*)	
238	6.5 ± 1.5	(α,2n)	(*50*)	4.4 ± 0.4 (*50*)
239	> 400	(α,3n)	(*52*)	
239	> 100	(α,3n), (α,n)	(*50*)	3.0 ± 0.2 (*50*)
239	8000	(d,p), (d,pn)	(*45*)	2.1 (*11*)
240	4.4 ± 0.8	(α,2n)	(*52*)	2.4 (*11*)
240	4.7 ± 0.6	(n,γ)	(*44*)	
240	3.8 ± 0.3	(α,2n)	(*50*)	3.0 ± 0.2 (*50*)
240	29 ± 4	(n,γ)	(*44*)	
241	30 ± 5	(d,p)	(*47*)	2.1 ± 0.2 (see text)
241	27,000	(d,p), (d,pn)	(*45*)	
241	10^{16}(?)	(n,γ)	(*7*)	
242	50 ± 30	(d,p)	(*47*)	
243	60 ± 15	(d,p)	(*47*)	≤ 3.3 (*11*)
		Americium		
237	5	(p,2n)	(*45*)	2.6 ± 0.3 (*45*, *51*)
238	60,000	(p,2n)	(*53*)	3 to 4
239	160 ± 40	(p,2n)	(*47*)	2.5 (*47*, *51*)
240	900,000	(p,2n)	(*6*, *26*)	3.15 ± 0.25 (*26*); 2.7 (*51*)
241	1500 ± 600	(p,2n)	(*47*)	2.1 (*47*, *51*)
242	14,000,000	Several	(*6*)	2.5 (*6*, *51*)
243	6500	(d,pn)	(*45*)	
244	1,100,000	Several	(*6*)	
		Curium		
240	< 2	(p,2n)	(*45*)	
241	19	(d,2n)	(*45*)	
241	20	(α,2n)	(*49*)	
242	< 2	(p,2n)	(*45*)	
243	38	(d,2n)	(*45*)	
243	45	(^{3}He,p)	(*49*)	

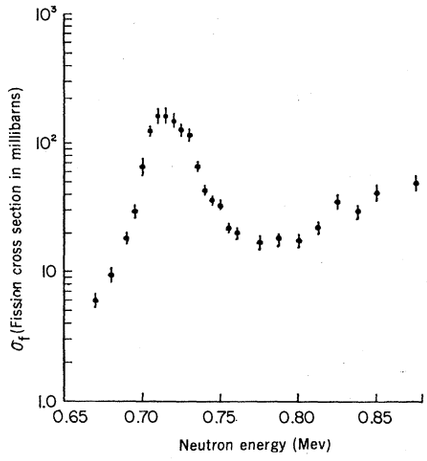

Fig. 3. The ^{230}Th(n,f) cross section as a function of neutron energy (*11*, *13*).

confirm this simple model with the $K = 0$ state at the lowest energy.

It has been known for some time that there is structure in the angular distributions of the fission fragments in the neutron fission (*18*) of even-even targets at energies near the barrier. This structure changes for some thorium and uranium isotopes over energy intervals of the order of 100 kiloelectron volts and is usually interpreted in terms of the Bohr model (*17*) with different K values of specific fission channels contributing near the barrier. An example is the fission of ^{234}U at

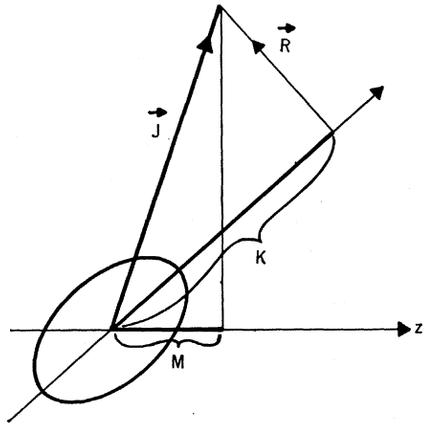

Fig. 4. Angular momentum coupling scheme for a deformed nucleus. The vector J defines the total angular momentum. The quantity M is the component of the total angular momentum on the space-fixed z-axis. I define this direction as the beam direction. The quantity K is the component of the total angular momentum along the axis of nuclear symmetry. The collective rotational angular momentum, R, is perpendicular to the nuclear symmetry axis; thus, K is entirely a property of the intrinsic motion. Angle θ is the angle between the z-axis and the symmetry axis of the nucleus along which K is measured.

several neutron energies (*19*); the angular distributions are shown in Fig. 5.

In the case of two barriers, the question arises as to which of the two barriers A or B is responsible for the structure. For the thorium and uranium isotopes the indication is that barrier B is higher and is associated with the structure. Near-barrier neutron-induced fission of heavier elements gives rather smooth angular distributions with weak forward peaking. If this difference in the character of the angular distributions of fragments is interpreted as a drastic change in the barrier shape with atomic weight, one would postulate that barrier A is higher for the heavier nuclei. If the second well is deep, the nucleus will pass through this region slowly enough so that the K value with which it passed over the first barrier is altered. The angular distribution may then reflect the K distribution at barrier B. If barrier B is sufficiently lower than barrier A, many channels may be open, thus resulting in a statistical distribution of K. Although the experimental data are consistent with this picture (*16*, *20*), such evidence for the double-humped barrier is rather indirect.

If one examines fission at energies in excess of the barrier, one expects angular distributions given by statistical theory with a Gaussian K distribution (*21*). The standard deviation of the Gaussian K distribution is directly related to the deformation of the transition nucleus. Measurements of the angular distributions of fragments over a large range of nuclei has demonstrated that the shape of the saddle point changes (*22*) in the direction predicted according to the liquid-drop model. However, these data indicate that the highest barrier may be changing from barrier B to barrier A somewhere in the vicinity of uranium.

Theoretical Basis for Double-Humped Barriers

There are marked deviations from the predictions of the liquid-drop model in the total nuclear binding energies in the vicinity of the well-known neutron and proton shells. Although the importance of shells for spherical nuclei has been recognized for some time, Strutinsky (*5*) has shown that the shell nonuniformities in the energy distribution of the nucleons are also important for deformed nuclei, as is evidenced by the fact that certain nuclei have deformed ground states. In his shell correction method Strutinsky ascribes equivalent effects to variations in the particle number and deformation. One is familiar with the variation of nuclear binding energies with particle number but much less familiar with the variation in energy with deformation. The density of single particle levels near the Fermi energy oscillates as a function of deformation, and this leads to modulations in the liquid-drop energy of a nucleus. When the density of single particle levels thins out near the Fermi energy, a typical shell is defined. Hence, the ground state of uranium is deformed because the nucleons in this nucleus arrange themselves most favorably in a deformed potential well to give the most stable deformation. The location of shells in the potential well is a function of both the single particle energy and the deformation β.

The total nuclear binding energy may be written as

$$E(Z,N,\beta) = E_{LD}(Z,N) + \Delta E(Z,N,\beta) \quad (2)$$

where $E_{LD}(Z,N)$ is the binding energy given by the liquid-drop model, $\Delta E(Z,N,\beta)$ is a correction term due to nuclear shells which is dependent on deformation β, and N represents neutron number. Strutinsky has developed a sensitive procedure for calculating the deformation-dependent correction term $\Delta E(Z,N,\beta)$. His method is based on an evaluation of the fluctuation of the density of the levels relative to the average density from the shell model with nonspherical potentials included. The final energy corrections also include pairing. In this pioneer work Strutinsky has checked his formalism by calculating the total nuclear binding energies of nuclear ground states. The shell correction method was used to evaluate the energy corrections of the ground state which include the effects due to the proton and neutron shells and to pairing for the equilibrium deformations. The success of these calculations in permitting one to predict the fluctuations of the nuclear binding energies of the ground state around the liquid-drop average values gives one confidence that the procedure is correct.

The magnitude of the shell correction is only a few million electron volts relative to a nuclear binding energy of the order of 1000 million electron volts. Such small energy corrections are important, however, because the fission barrier itself is only

some 5 million electron volts. Calculation of the potential energy surface in the vicinity of the fission barrier requires that one use the shell correction method to determine the change in energy with the variation in nuclear deformation. On the basis of such a calculation, the first minimum in the potential energy is located at the known deformation of the nuclear ground state. Of particular interest for an understanding of nuclear fission is the fact that the second minimum is in the vicinity of the saddle point deformation. The minima at these deformations are associated with a lower density of levels near the Fermi energy. The first minimum arises from crossings of single particle levels from major oscillator shells N and $N \pm 1$, whereas the second minimum arises from similar crossings of the N and $N \pm 2$ oscillator levels. The usefulness of the Strutinsky method for computing the structure in the fission barrier rests on the renormalization procedure at each deformation with a liquid-drop energy that is very large relative to the shell correction energy. Attempts to calculate the barrier energy as a function of deformation with sophisticated shell models alone have thus far been unsuccessful.

The predicted existence of the second minimum according to the Strutinsky method is a regular feature independent of the choice of single particle model. Even when one uses rather different single particle models, including the finite-depth Woods-Saxon model (*23*), with the shell correction method, the results are similar. The presence of the second well is also unchanged by the inclusion of deformations of higher order such as P_4 deformations (*24*), nonaxially symmetric deformations (gamma-deformations), and octupole deformations (P_3) (*25*).

Semiquantitative Features of a Double-Humped Fission Barrier

In Fig. 1 a schematic representation is given of the intrinsic excitations at the two barriers and in the two potential wells. There are two different sets of equilibrium states in the compound nucleus, each with its own spectrum and properties. If a nucleus is excited by some reaction, its collective motion is quickly damped over the other degrees of freedom and the nucleus falls into one or the other of the two minima.

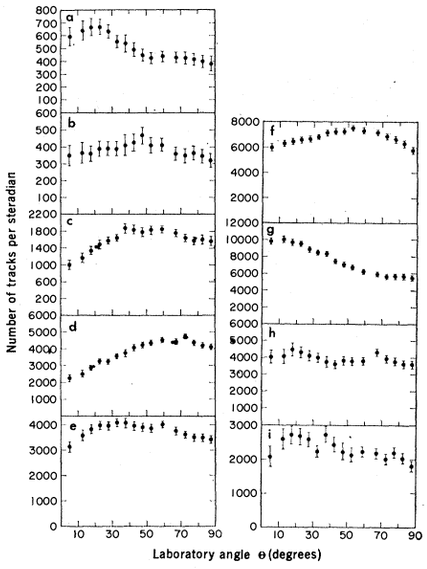

Fig. 5. Angular distributions of the fission fragments for the ^{234}U(n,f) reaction at the following incident neutron energies (in kiloelectron volts): (a) 200; (b) 300; (c) 400; (d) 500; (e) 600; (f) 700; (g) 843; (h) 998; (i) 1184 (*19*). The ordinate is proportional to the number of tracks or fission events observed at laboratory angle θ.

Fission induced with subbarrier monoenergetic neutrons gives direct information about the states in the second well. The structure in the cross section of ^{240}Pu (see Fig. 2) is schematically illustrated in Fig. 6. In Fig. 6 the total width γ_2^t of the states in the second well is larger than the total width of the compound nucleus Γ_t but smaller than the spacing D_{II} between levels in the second well. The spacing between the class II states, D_{II}, is much larger than the spacing between class I states, D_I. The area of each resonance state determines the fission width Γ_f.

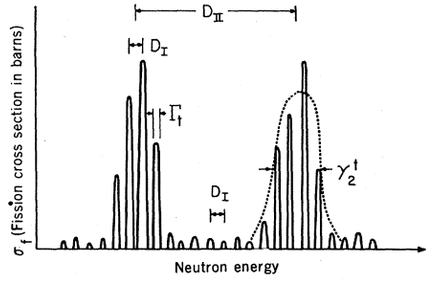

Fig. 6. Schematic illustration of the quantities that are important in the determination of the resonance cross section for the fission of ^{240}Pu with subbarrier neutrons (*16*). The quantities D_I and D_{II} are the spacings between class I and class II states respectively, Γ_t is the total width of the compound nucleus formed in neutron capture, and γ_2^t is the total width of the class II state.

For the case where the density of the levels in each well is large and the statistical model is valid, Bjørnholm and Strutinsky (*16*) derived the average fission width in the region of the resonance state of the second well

$$\langle \Gamma_f \rangle \approx \frac{\langle D_I \rangle}{2\pi} \frac{N_A N_B}{N_A + N_B} \qquad (3)$$

where N_A and N_B are the effective numbers of channels at barriers A and B, respectively. The spreading width γ_2^t of the states in the second well is given approximately by

$$\gamma_2^t \approx \frac{\langle D_{II} \rangle}{2\pi} (N_A + N_B) \qquad (4)$$

In the case of the subbarrier neutron fission resonance states observed with a ^{240}Pu target, the experimental values of $\langle D_I \rangle$, $\langle D_{II} \rangle$, $\langle \Gamma_f \rangle$, and γ_2^t are 15, 650, 0.040, and 50 electron volts (*9*, *16*), respectively. The solution of Eqs. 3 and 4 gives values for N_A (or N_B) of 0.47 and for N_B (or N_A) of 0.02. These results show that the energy is near the top of the barrier for either barrier A or barrier B. If barrier B is the higher barrier ($N_A = 0.47$ and $N_B = 0.02$), there is a relatively strong mixing of each intermediate state with the compound nuclear states and, as a result, each intermediate state is distributed among the observed resonance states in each group. On the other hand, if barrier A is higher ($N_A = 0.02$ and $N_B = 0.47$), then there is only weak coupling between the compound and intermediate states. In this case all the observed resonance states in the fission cross section are almost pure compound states and the intermediate state does not show up in other reaction channels because of its large fission width. From the neutron fission resonance data alone it is not possible to choose between these two possibilities and to conclude which of the two barriers is the higher barrier.

One may estimate the depth of the second potential well by comparing the density of class I and class II states. If the energy dependence of the density of the levels in each well is assumed to be the same, the ratio of level spacings in the two wells is given by the Fermi gas formula for the level density to be

$$\langle D_{II} \rangle / \langle D_I \rangle = (U_{II}/U_I)^{3/2} \exp\left[2a^{1/2}(\sqrt{U_I} - \sqrt{U_{II}})\right] \qquad (5)$$

where U_I and U_{II} are the excitation energies in the potential wells I and II, respectively, and a is the Fermi gas

level density parameter. In the case of the subbarrier neutron resonances of ^{240}Pu, $\langle D_{II}\rangle = 650 \pm 200$ electron volts, $\langle D_I\rangle = 15$ electron volts, $U_I = 5.4$ million electron volts (binding energy of a neutron fired at a ^{240}Pu atom, thus forming excited ^{241}Pu) and $a =$ 20 reciprocal million electron volts. From Eq. 5 one determines that the energy of the second potential minimum at deformation β_1 is $(U_I - U_{II}) = 2.1 \pm 0.2$ million electron volts. Values of the second potential minimum have been determined also for isomers of americium from excitation functions of the isomeric states. An example of such an excitation function (*26*) is given in Fig. 7 for the reaction ^{241}Pu(p,2n)^{240m}Am. The difference between the thresholds for the ground state and for the isomeric state is a measure of the excitation energy of the minimum in the second potential well at deformation β_1. On the basis of such a threshold measurement the value of $(U_I - U_{II})$ for the isomer of ^{240}Am is 3.15 million electron volts. The value of the energy minimum in the second well for ^{242}Am has been evaluated both by the threshold method and by the level spacing method of Eq. 5, and the agreement in the results is very good (*11*).

The ground and first excited class II vibrational states are essentially unmixed with more complex class II states and may be treated as one-dimensional states bounded by potential barriers A and B (Fig. 1). If the states in the first well are regarded as a continuum, the penetration for energies near the resonance energy can be computed as that of a free wave through a two-humped barrier. The penetration factor $P(E)$ for such a barrier is given by (*11*)

$$P(E) = \frac{P_A P_B}{(2\pi/D\nu)^2(E - E\nu)^2 + 1/4(P_A + P_B)^2} \quad (6)$$

where $E\nu$ and $D\nu$ are the vibrational state energy and spacing in the second well, respectively. The quantities P_A and P_B are the penetrabilities through parabolic (*27*) barriers A and B defined by

$$P_i = \{1 + \exp[2\pi(V_i - E\nu)/\hbar\omega_i\}]^{-1} \quad (7)$$

where V_i is the height of the barrier, $\hbar\omega_i$ is an energy defining the barrier curvature, and i refers to either barrier A or barrier B.

Equation 6 makes it clear that the penetration function for a two-humped barrier may no longer be thought of as a smooth function of E; rather the penetration function must be thought of as a function with sharp maxima at the energies corresponding to the energies of the vibrational states in the second well. The half-width of each maximum is determined by the lifetime of the corresponding level in the second well, which, in turn, is determined by the penetrabilities of barriers A and B. In order that one understand the consequences of a two-humped barrier, it is useful to examine the results obtained with Eq. 6. At the resonance energy $E = E\nu$, Eq. 6 reduces to

$$P_{max} = 4P_A P_B/(P_A + P_B)^2 \quad (8)$$

If the two barriers A and B are symmetrical and P_A equals P_B, then the penetrability tends toward unity even though the energy of the vibrational state is well below that of the barriers. In the general case of unsymmetrical barriers the penetrability of one barrier will be small relative to that of the other such that $P_{max} = 4P_B/P_A$ (for case $P_B \ll P_A$). At energies far from the resonance energy, the penetration is given approximately by the product of the two penetrabilities, $P(E) \approx P_A P_B$.

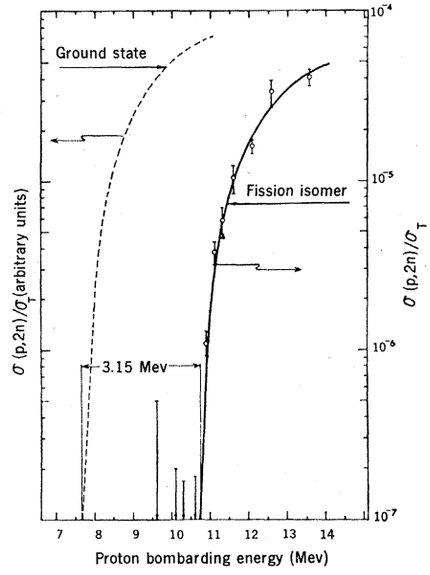

Fig. 7. Plot (*26*) of the ratio of the cross section σ(p,2n) for production of the isomer ^{240m}Am by the ^{241}Pu(p,2n)^{240m}Am reaction to the total reaction cross section σ_T (open circles and solid line) as a function of proton bombarding energy. The dashed line gives the ratio of the cross section σ(p,2n) for production of the ground state ^{240}Am by the ^{241}Pu(p,2n) ^{240}Am reaction to the total reaction cross section σ_T.

A qualitative comparison of the penetrabilities of one- and two-humped fission barriers is illustrated in Fig. 8. Whereas the penetrability for a single-humped parabolic barrier increases smoothly with energy from a value near zero to a value near unity with a value of ½ at the barrier energy, the two-humped barrier has built on this smooth trend a strong resonance structure corresponding to the energies of the vibrational levels in the second well. The resonances observed in the ^{230}Th(n,f) reaction at 700 kiloelectron volts and in the (d,pf) reactions may be due to this unusual feature of maxima in the penetration of a two-humped barrier.

Direct information about the two barriers may be deduced from the half-lives for spontaneous fission decay of the ground and isomeric states. Whereas the isomeric lifetime is a measure of the penetration through the second barrier B, the fission lifetime of the ground state is a measure of the penetration of both barriers A and B (at a different energy). If one assumes a parabolic barrier and a mean lifetime related to the barrier penetrability by

$$T_{s.f.} = \left(\frac{C}{2\pi} P\right)^{-1}$$

where $C/2\pi$ is the frequency of assaults on the barrier of 4×10^{20} per second, the value of $[E_f(B) - E_{II}]\hbar\omega$ may be calculated from Eq. 7 if the isomeric fission lifetime is known. The quantities $E_f(B)$ and E_{II} are the height of barrier B and the energy of the isomeric state, respectively. The energy of the isomeric state is known for some nuclei from measurements of the kind discussed earlier in this section. However, the lifetime alone does not allow one to determine $E_f(B)$ and $\hbar\omega$ separately. In practice, an estimate of the value of one or the other quantity is made from other information and then the remaining parameter is determined. Although the indices for the quantum numbers are omitted for simplicity, the penetration for each channel, which is characterized by its own quantum numbers and energies, must be determined individually.

Bjørnholm and Strutinsky (*16*) have discussed the relation between the half-lives for spontaneous fission decay of the ground and isomeric states in terms of two models with parabolic barriers. In the first model a double-humped

barrier is constructed with parabolic segments joined at an energy equal to the isomer energy, E_{II}. The heights of barriers A and B are assumed to be equal and are given the value of the experimental barrier. From the two experimental values of the half-lives the quantities $\hbar\omega_A$ and $\hbar\omega_B$ are determined. In the second model it is assumed that $\hbar\omega_A$ is equal to $\hbar\omega_B$ and that $E_f(B)$ is equal to the experimental barrier; then the values of $\hbar\omega_B$ and $E_f(A)$ are determined from the lifetime data. Results of calculations based on the first model require $\hbar\omega$ to be of the order of 0.6 to 0.8 million electron volts and $\hbar w_A$ to be slightly larger than $\hbar\omega_B$, whereas the results of calculations based on the second model with barrier A lower than barrier B are in conflict with other data for these nuclei.

Scission

Heavy nuclei near uranium in the periodic table fission asymmetrically to give light and heavy fragments with the most probable masses in the vicinity of mass numbers 96 and 140, respectively. This early experimental result has been one of the more difficult puzzles for fission theorists to explain. Although various explanations based on the effects of nuclear shells either in the transition-state nucleus or in the primary fragments have been proposed, no satisfactory theory has been developed to date.

With the availability of large computers, extensive calculations based on the liquid-drop model have been performed over the last few years in order to map out the potential energy surface of heavy nuclei as a function of their deformation. The saddle point or transition-state deformation (*3*) has been located for different nuclei and its properties have been studied thoroughly. However, these early calculations gave symmetric shapes for the saddle point. Recently, more realistic theoretical calculations incorporating the Strutinsky shell correction along with the inclusion of P_3 (pear-shaped deformation) and higher order asymmetric deformation (P_5) indicate that the saddle configuration is asymmetric (*28*). If these results are confirmed and the nucleus in its transition state is asymmetrically deformed, this will truly be an exciting development in fission and an important contribution to the explanation of asymmetric fission.

If, however, the results of more accurate calculations of the potential energy show that the saddle configuration is stable to asymmetric deformations, one may still postulate that asymmetric instabilities develop on the path from the saddle to the scission configuration. To theoretically test this possibility, accurate shell corrections for very large deformations must be added to the liquid-drop energies. The use of statics in tracing out the lowest potential energy surface as a function of deformation all the way to the scission shape is of extreme importance. However, precise results depend on new experimental data and computational techniques, such as the Strutinsky method for shell correction.

Theoretical attempts to understand asymmetric fission, with the inclusion of the dynamics also, have developed on the basis of two different fundamental assumptions. In the "statistical theories" it is assumed that there is a viscous liquid drop with a strong cou-

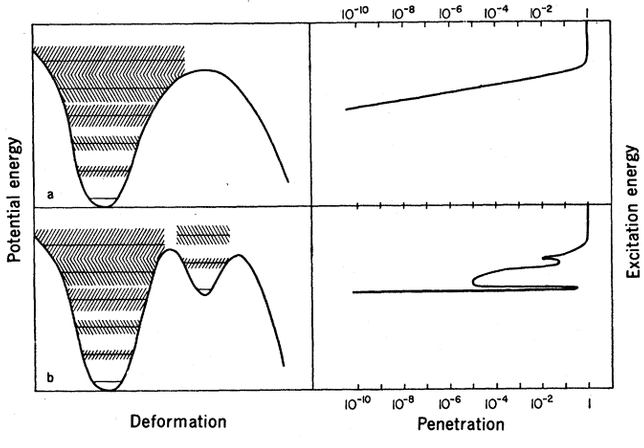

Fig. 8 (left). Schematic comparison of the penetrability functions for vibrational states in (a) a single-well and (b) a double-well model (*16*). The heavy lines represent vibrational states that are approximately 1 million electron volts apart in the absence of damping. Damping is indicated by the hatched lines where in the first well at the higher energies the vibrational states form a continuum. Note the spikes in the penetrability function for the two-well model when the excitation energy corresponds to the energy of a vibrational state in the second well. Fig. 9 (upper right). Average total kinetic energy as a function of heavy fragment mass (*34*). The dip in the kinetic energy near symmetry is slightly exaggerated because the data have not been corrected for fission fragment scattering. (Open circles) Experimental; (filled circles) calculated. Fig. 10 (lower right). Neutron yields (*35*) ν_L and ν_H as a function of the mass of the light and heavy fission fragment, respectively. Also shown are the approximate initial fragment masses corresponding to various neutron and proton "magic numbers."

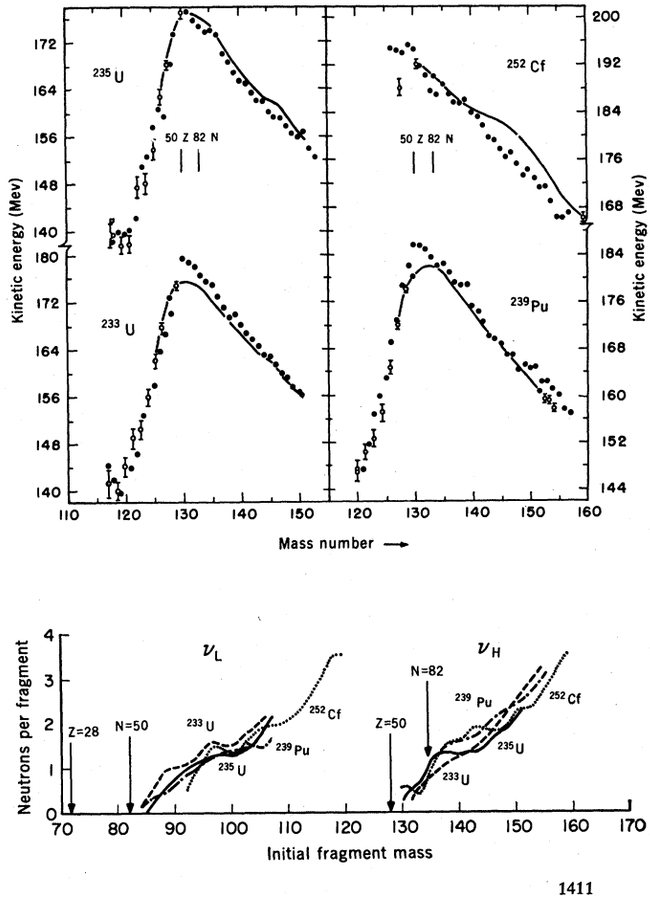

pling between the collective and internal degrees of freedom, thus ensuring statistical equilibrium during the motion from the saddle point to scission. In this model (*29*) the probability distributions of all the various properties of the fragments, such as the fragment masses, excitation energies, and angular distributions, are a direct result of the equilibrium at scission. The other extreme assumption is that the coupling between the collective and internal motions is weak, and this model is sometimes referred to as the adiabatic model (*30*). In the first model the properties of the saddle point are not allowed to influence the results at scission. Hence, on the basis of this model, it is difficult to understand the angular distributions of the fission fragments which are known to reflect the K distribution of the transition-state nucleus. On the other hand, in a simplified version of the second model based on the nonviscous irrotational liquid drop it is assumed that the model possesses "memory" of the transition-state properties although in this model there is no capability to reproduce the observed mass asymmetry.

Beginning with the assumption that the shape of the saddle point and the lowest potential energy surface to scission are symmetric, various authors (*31*), in searching for an explanation of asymmetric fission, have suggested that the final mass ratio is a result of reflection symmetry. In this model the collective motion between saddle point and scission is so rapid that equilibrium is not attained. As the nuclear shape changes through the value where a filled independent particle level is crossed by an unfilled level, the probability that the nucleons will remain in the lower energy orbit is small. This is in contrast to the result for slow collective motion where the probability that the nucleons will remain in the lowest energy orbital is large. Hence, in this model with slow collective motion the nuclear deformation follows the lowest valley of potential energy and leads to symmetric fission. On the other hand, with fast collective motion the nuclear deformation follows a potential surface generated when particle transfer is forbidden at level crossings and leads to asymmetric fission. In the development of this model Griffin (*32*) has proposed the principle of "kinetic dominance" as the basis for predicting the rapid collective motion, namely, "in the limit of high collective velocity, nuclear shape changes are described by a potential energy surface defined by the energies of nuclear configurations which are deformed into one another with a minimal collective inertia." Motion along the lowest potential energy surface involves a continual readjustment of nucleons so that the lowest energy orbitals are always occupied, thus giving a substantial contribution to the collective inertia. In contrast, motion along a potential energy surface at which the nucleons do not readjust their orbitals gives a smaller inertial parameter comparable to the irrotational value. On this basis asymmetric mass division is predicted. Although this model has appealing features, its need at this time is not established since it is still unknown whether the lowest potential energy surface from the saddle point to scission deformation is symmetric or asymmetric. More realistic and accurate shell corrections are needed to settle this question.

In order to explain the kinetic energy and neutron emission as a function of fragment mass, Vandenbosch (*33*) proposed that the most probable scission configuration has a minimum potential energy. With the further assumption that the scission configuration is represented by two uniformly charged tangent spheroids, the potential energy is given by a sum of the deformation energies of each fragment and the Coulomb energy between the two fragments. The deformation energy of each fragment is represented by the deformation energy of a charged liquid drop and a correction term dependent upon the nuclear structure of the fragment. The influence of nuclear shells introduces structure into the kinetic energy (*34*) and neutron emission yield (*35*) as a function of fragment mass. The experimental kinetic energies for the neutron-induced fission of ^{233}U, ^{235}U, and ^{239}Pu have a pronounced dip as symmetry is approached. These results are shown in Fig. 9. The variation in the neutron yield as a function of fragment mass for these same nuclei (Fig. 10) has a "saw-toothed" shape which is asymmetric about the symmetric fission fragment mass. Both of these phenomena are reasonably well accounted for by the inclusion of closed-shell structure (*33*) into the scission configuration.

A number of light charged particles have been observed to occur in fission with low probability (*36, 37*). These particles are believed to be emitted very near the time of scission and hence are of extreme interest. The evidence for these particles being emitted near the scission stage comes mainly from detailed studies of the alpha particles accompanying fission (*38*). Available evidence also indicates that neutrons are emitted at or near scission with considerable frequency (*39*).

Experimental studies have been made of the kinetic energy and angular distributions of the light charged particles. In addition, studies have been made of the correlations between the energy and emission angle of the light particle, between the fragment and particle energies, and between the angle of particle emission and the fragment mass ratio (*40*). Calculations (*37, 38, 41*) aimed at reproducing the experimental observations indicate that the equilibrium model giving an essentially static picture of scission is incorrect. Instead the calculations support a dynamic picture of scission in which the fragments are moving apart at scission with an appreciable fraction ($\sim$¼) of their final kinetic energy.

The most probable kinetic energy calculated for an idealized nonviscous irrotational liquid drop is considerably less (*42*) than the experimentally determined most probable kinetic energy of the fission fragments. The difference is well represented by the kinetic energy that the fragments have acquired at scission as determined by the alpha particles accompanying fission. These results are of significance in the evaluation of the viscosity of nuclear matter.

Postscission Phenomena

Many experiments have been designed to investigate postscission phenomena. After the fragments are separated at scission, they are further accelerated as a result of the large Coulomb repulsion. The fragments reach 90 percent of their final kinetic energies in approximately 10^{-20} second. The initially deformed primary fragment probably collapses to its equilibrium shape in a time period shorter than this. The time for neutron evaporation is long relative to the time for fragment acceleration, and the evaporated neutrons are emitted from the fully accelerated fragments. The evap-

orated neutrons comprise most of the neutron yield in fission. (The scission neutrons are estimated to comprise as much as 30 percent of the neutron yield (*39*), whereas the delayed neutrons produced after beta decay comprise only about 0.2 to 0.6 percent of the neutron yield. Isomeric fission offers a new source of delayed neutrons of very low intensity.) The fragments, after neutron emission, lose the remainder of their energy by gamma radiation with a lifetime of about 10^{-11} second.

The neutron yield as a function of mass number is illustrated in Fig. 10. This variation of neutron number N with fragment mass (*35*) has been studied rather extensively because of its relation to the fragment excitation energy. The resulting functions are "saw-toothed" and asymmetric about the symmetric fragment mass. Minimum neutron yields are observed for nuclei near closed shells because of the resistance of nuclei with closed shells to deformation. Maximum neutron yields occur for fragments that are "soft" toward nuclear deformation. Hence, at the scission configuration the fraction of the deformation energy stored in each fragment depends on the shell structure of the individual fragments. After scission this deformation energy is converted to excitation energy and, hence, the neutron yield is directly correlated with the fragment shell structure. This conclusion is further supported by the correlation between the neutron yield and the final kinetic energy. Closed shells result in a larger Coulomb energy at scission for fragments that have a smaller deformation energy and a smaller number of evaporated neutrons.

The relative yield (*43*) of prompt gamma rays as a function of fragment mass is very similar to the relative yield of neutrons. The high multiplicity of gamma rays from one fragment is connected with a low multiplicity in the complimentary fragment. This result implies a large difference in spin angular momentum in the two fragments and is consistent with the presence of shell structure in one fragment.

Conclusion

Nuclear shells play a significant role in nuclear fission. Although the importance of nuclear shells in the scission and postscission stages of fission has been known for some time, recent work has shown that nuclear shells introduce structure into the fission barrier also, thus causing a second minimum in the potential energy at the saddle point deformation. This two-humped fission barrier is essential for the explanation of the fission isomers, subbarrier fission resonances, and other anomalies observed in fission. Nuclear fission is a complex and basic nuclear reaction, and clarification of its nature is essential to our understanding of the dynamics of heavy nuclei. The study of fission gives one the unique opportunity to probe the properties of nuclear structure as a function of deformation out to very large deformations and to learn about the shape dependence of the nuclear potential energy.

References and Notes

1. O. Hahn and F. Strassmann, *Naturwissenschaften* **27**, 11 (1939).
2. N. Bohr and J. A. Wheeler, *Phys. Rev.* **56**, 426 (1939).
3. S. Cohen and W. J. Swiatecki, *Ann. Phys. N.Y.* **19**, 67 (1962); *ibid.* **22**, 406 (1963); V. M. Strutinsky, N. Ya. Lyashschenko, N. A. Popov, *Nucl. Phys.* **46**, 639 (1963).
4. W. D. Myers and W. J. Swiatecki, *Nucl. Phys.* **81**, 1 (1966).
5. V. M. Strutinsky, *ibid.* **A95**, 420 (1967); *ibid.* **A122**, 1 (1968).
6. S. M. Polikanov, *Usp. Fiz. Nauk* **94**, 43 (1968).
7. R. Nisle, I. Stephen, C. Reich, results mentioned in paper by S. G. Nilsson, G. Ohlén, C. Gustafson, P. Möller, *Phys. Lett.* **30B**, 437 (1969).
8. F. H. Ruddy and J. M. Alexander, *Phys. Rev.* **187**, 1672 (1969).
9. E. Migneco and J. P. Theobald, *Nucl. Phys.* **A112**, 603 (1968).
10. H. Weigmann, *Z. Phys.* **214**, 7 (1968).
11. J. E. Lynn, in *Symposium on the Physics and Chemistry of Fission* (International Atomic Energy Agency, Vienna, 1969), p. 249.
12. P. E. Vorotnikov, S. M. Dubrovina, V. A. Shigin, G. A. Otroschenko, *Sov. J. Nucl. Phys. Engl. Transl.* **5**, 210 (1967).
13. L. Earwaker and G. D. James, results reported in reference (*11*).
14. J. Pedersen and B. P. Kuzminov, *Phys. Lett.* **29B**, 176 (1969).
15. H. J. Specht, J. S. Fraser, J. C. D. Milton, W. G. Davies, in *Symposium on the Physics and Chemistry of Fission* (International Atomic Energy Agency, Vienna, 1969), p. 363.
16. S. Bjørnholm and V. M. Strutinsky, *Nucl. Phys.* **A136**, 1 (1969).
17. A. Bohr, *Proc. Int. Conf. Peaceful Uses At. Energy, Geneva, 1955* **2**, 151 (1955).
18. R. W. Lamphere, in *Symposium on the Physics and Chemistry of Fission* (International Atomic Energy Agency, Vienna, 1965), vol. 1, p. 63.
19. A. N. Behkami, J. H. Roberts, W. Loveland, J. R. Huizenga, *Phys. Rev.* **171**, 1267 (1968).
20. K. Otozai, J. W. Meadows, A. N. Behkami, J. R. Huizenga, *Nucl. Phys.* **A144**, 502 (1970).
21. I. Halpern and V. M. Strutinsky, *U.N. Proc. Int. Conf. Peaceful Uses At. Energy, 2nd Geneva, 1958* **15**, 1513 (1958).
22. R. F. Reising, G. L. Bate, J. R. Huizenga, *Phys. Rev.* **141**, 1161 (1965).
23. V. M. Strutinsky and H. C. Pauli, in *Symposium on the Physics and Chemistry of Fission* (International Atomic Energy Agency, Vienna, 1969), p. 155.
24. S. G. Nilsson, C. F. Tsang, A. Sobiczewski, Z. Szymanski, S. Wycech, C. Gustafson, I. L. Lamm, P. Möller, B. Nilsson, *Nucl. Phys.* **A131**, 1 (1969).
25. V. V. Pashevich, paper presented at the International Symposium on Nuclear Structure, Dubna, 1968, preprint D-3893, p. 94.
26. S. Bjørnholm, J. Borggreen, L. Westgaard, V. A. Karnauchov, *Nucl. Phys.* **A95**, 513 (1967).
27. D. L. Hill and J. A. Wheeler, *Phys. Rev.* **89**, 1102 (1953).
28. P. Möller and S. G. Nilsson, *Phys. Lett.* **31B**, 283 (1970).
29. P. Fong, *Statistical Theory of Nuclear Fission* (Gordon & Breach, New York, 1968).
30. L. Wilets, *Theories of Nuclear Fission* (Oxford Univ. Press, New York, 1964).
31. I. Kelson, *Phys. Rev. Lett.* **20**, 867 (1968); J. J. Griffin, *ibid.* **21**, 826 (1968).
32. J. J. Griffin, *Univ. Maryland Center Theor. Phys. Rep. No. 70-009* (August 1969).
33. R. Vandenbosch, *Nucl. Phys.* **46**, 129 (1963).
34. J. D. C. Milton and J. S. Fraser, *Can. J. Phys.* **40**, 1626 (1962).
35. J. Terrell, in *Symposium on the Physics and Chemistry of Fission* (International Atomic Energy Agency, Vienna, 1965), vol. 2, p. 3.
36. S. L. Whetstone, Jr., and T. D. Thomas, *Phys. Rev.* **154**, 1174 (1967); S. W. Cosper, J. Cerny, R. C. Gatti, *ibid.*, p. 1193.
37. G. M. Raisbeck and T. D. Thomas, *ibid.* **172**, 1272 (1968).
38. I. Halpern, in *Symposium on the Physics and Chemistry of Fission* (International Atomic Energy Agency, Vienna, 1965), vol. 2, p. 369.
39. J. C. D. Milton and J. S. Fraser, *ibid.*, p. 39.
40. Z. Fraenkel and S. G. Thompson, *Phys. Rev. Lett.* **13**, 438 (1964).
41. V. Boneh, Z. Fraenkel, I. Nebenzahl, *Phys. Rev.* **156**, 1305 (1967); A. Katase, *J. Phys. Soc. Jap.* **25**, 933 (1968).
42. J. R. Nix, *Univ. Calif. Radiat. Lab. Rep. No. UCRL-17958* (1968).
43. S. A. E. Johansson, *Nucl. Phys.* **60**, 378 (1964).
44. A. J. Elwyn and A. T. G. Ferguson, *Nucl. Phys.*, in press.
45. S. M. Polikanov and G. Sletten, *ibid.*, in press.
46. K. L. Wolf, R. Vandenbosch, P. A. Russo, M. K. Mehta, C. R. Rudy, *Phys. Rev.*, in press.
47. N. L. Lark, G. Sletten, J. Pedersen, S. Bjørnholm, *Nucl. Phys.* **A139**, 481 (1969).
48. R. Repnow, V. Metag, J. D. Fox, P. von Brentano, in preparation.
49. V. Metag, R. Repnow, P. von Brentano, J. D. Fox, in *Symposium on the Physics and Chemistry of Fission* (International Atomic Energy Agency, Vienna, 1969), p. 449.
50. S. C. Burnett, H. C. Britt, B. H. Erkkila, W. E. Stein, *Phys. Lett.* **31B**, 523 (1970).
51. S. Jägare, *Nucl. Phys.*, in press.
52. R. Vandenbosch and K. Wolf, in *Symposium on the Physics and Chemistry of Fission* (International Atomic Energy Agency, Vienna, 1969), p. 439.
53. J. Borggreen, Y. P. Gangrsky, G. Sletten, S. Bjørnholm, *Phys. Lett.* **25B**, 402 (1967).

54. I thank Professors H. M. Blann, H. E. Gove, and K. G. Harbison for a critical reading of the manuscript. I acknowledge helpful comments from Drs. S. Bjørnholm, H. C. Britt, J. P. Unik, and R. Vandenbosch in the preparation of Table 1. Supported by the U.S. Atomic Energy Commission.